

Hydrogen fuelled scramjet combustor - the impact of fuel injection

Wei Huang^{1,2}, Zhen-guo Wang¹, Mohamed Pourkashanian²,
Lin Ma², Derek B.Ingham², Shi-bin Luo¹ and Jun Liu¹

¹College of Aerospace and Materials Engineering, National University of Defense
Technology, Changsha, Hunan, People's Republic of China, 410073

²Centre for CFD, School of Process, Environmental and Materials Engineering,
University of Leeds, United Kingdoms, LS2 9JT

1. Introduction

The scramjet engine is one of the most promising propulsive systems for future hypersonic vehicles. Over the last fifty years the scramjet engine technology has been intensively investigated and several such engines have been flight-tested in recent years (Neal, Michael, & Allan, 2005; Paul, Vincent, Luat, & Jeryl, 2004). Research on supersonic combustion technologies is of great significance for the design of the engine and many researchers pay significant attention to the hypersonic airbreathing propulsion. The mixing and diffusive combustion of fuel and air in conventional scramjet engines take place simultaneously in the combustor (Huang, Qin, Luo, & Wang, 2010). Since the incoming supersonic flow can stay in the combustor only for a very short period of time, i.e. of the order of milliseconds (Aso, Inoue, Yamaguchi, & Tani, 2009; Huang *et al.*, 2010; Hyungseok, Hui, Jaewoo, & Yunghwan, 2009), and the whole process of combustion has to be completed within this short duration, this is a significant restriction to the design of the scramjet engine. In order to solve this problem, hydrogen, one of the most promising fuels for the airbreathing engine with ~10 times faster reaction than hydrocarbons, is widely used in the scramjet combustor.

In recent years, a cavity flameholder, which is an integrated fuel injection/flame-holding approach, has been proposed as a new concept for flame holding and stabilization in supersonic combustors (Alejandro, Joseph, & Viswanath, 2010; Chadwick *et al.*, 2005; Chadwick, Sulabh, & James, 2007; Daniel & James, 2009; Gu, Chen, & Chang, 2009; Jeong, O'Byrne, Jeung, & Houwong, 2008; Kyung, Seung, & Cho, 2004; Sun, Geng, Liang, & Wang, 2009; Vikramaditya & Kurian, 2009). The presence of a cavity on an aerodynamic surface could have a significant impact on the flow surrounding it. The flow field inside a cavity flameholder is characterized by the recirculation flow that increases the residence time of the fluid entering the cavity, and the cavity flame provides a source of heat and radicals to ignite and stabilize the combustion in the core flow.

However, so far, the flow field in the scramjet combustor with multiple cavity flameholders has been rarely discussed, and this is an important issue as it can provide some useful guidance for the further design of the scramjet combustor. Multi-cavity flameholder can

produce larger drag forces on the scramjet combustor, as well as improve the combustion efficiency of the combustor. A balance between these two aspects will be very important in the future design of the propulsion system in hypersonic vehicles. At the same time, the combustor configuration, i.e. the divergence angle of each stage, makes a large difference to the performance of the combustor. Researchers have shown that (Huang, Li, Wu, & Wang, 2009) the effect of the divergence angles of the posterior stages on the performance of the scramjet combustor is the most important, and the effect of the divergence angle on the first stage is the least important. When the location of the fuel injection moves forward, the effect of the divergence angle of the former stages becomes more important.

In this chapter, the two-dimensional coupled implicit Reynolds Averaged Navier-Stokes (RANS) equations, the standard $k-\epsilon$ turbulence model (Huang & Wang, 2009; Launder & Spalding, 1974) and the finite-rate/eddy-dissipation reaction model (Nardo, Calchetti, Mongiello, Giammartini, & Rufoloni, 2009) have been employed to investigate the effect of the location of the fuel injection on the combustion flow field of a typical hydrogen-fueled scramjet combustor with multi-cavities.

2. Physical model and numerical method

The engine investigated adopts the single-expanded combustor and fractional combustion mode, and it consists of an isolator and three staged combustors, see Fig. 1. There are four cavity flame holders located on the upper and lower walls of the first and the second staged combustors, respectively. Hydrogen is injected from the slot, located at 5mm from the leading edge of the four cavity flame holders on both the upper and lower walls of the first and the second staged combustor. The width of the slot is 1mm.

Assuming that the height of the isolator H_i is 1 unit, the distance between the upstream forward face of the cavity flameholder in the upper wall and that in the lower wall of each staged combustor is 0.183 along the x axis. The dimensions of the components of the scramjet combustor are shown in Table.1, where L_i , L_{c1} , L_{c2} and L_{c3} are the lengths of the isolator, the first staged combustor, the second staged combustor and the third staged combustor, respectively. The divergence angles of the first staged combustor, β_1 , the second staged combustor, β_2 and the third staged combustor, β_3 are 2.0 degree, 3.5 degree and 4.0 degree, respectively.

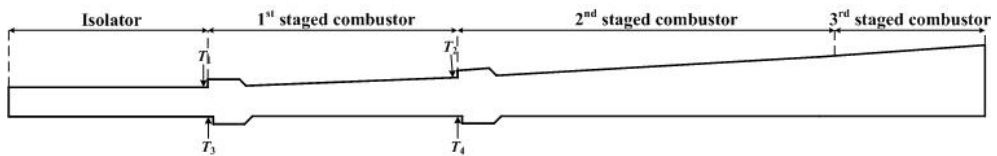


Fig. 1. A schematic of a typical scramjet combustor that has been investigated.

H_i	L_i	L_{c1}	L_{c2}	L_{c3}	$\beta_1/(\circ)$	$\beta_2/(\circ)$	$\beta_3/(\circ)$
1.0	7.0	8.8	12.8	5.8	2.0	3.5	4.0

Table 1. Geometrical dimensions of the scramjet combustor.

The primary geometry parameters of the cavity flameholder: the length of the cavity flameholder $L=1.376$, the height of the leading edge $D_u=0.275$, the ratio of length-to-height

$L/D_u=5.0$, the swept angle $\theta=45^\circ$ and the height of the trailing edge $D_d=0.275$. A schematic diagram of a typical cavity flameholder that has been investigated is shown in Fig. 2.

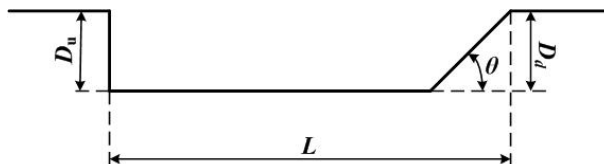


Fig. 2. A schematic of a typical cavity flameholder that has been investigated.

Table.2 shows the boundary conditions employed in the computational fluid dynamics (CFD) models. The ratio of the oxygen gas mol fraction to the nitrogen gas mol fraction at the entrance of the combustor is 23:77, with the Mach number being 3.2, the total pressure 2.9MPa and the total temperature 1505.0K. The hydrogen is injected into the core flow with sonic velocity, as shown in Table.2. The static pressure and temperature of the injection are 1060KPa and 250K, respectively.

	Ma	P_e/KPa	T_e/K	Y_{N_2}	Y_{O_2}	Y_{H_2}
The entrance of the combustor	3.2	58.66	493.77	0.77	0.23	0
The exit of the injection	1.0	1060	250	0.0	0.0	1.0

Table 2. Boundary conditions for the numerical model.

In the CFD model, the standard $k-\epsilon$ turbulence model is selected. This is because of its robustness and its ability to fit the initial iteration, design lectotype and parametric investigation. Further, because of the intense turbulent combustion effects, the finite-rate/eddy-dissipation reaction model is adopted. The finite-rate/eddy dissipation model is based on the hypothesis of infinitely fast reactions and the reaction rate is controlled by the turbulent mixing. Both the Arrhenius rate and the mixing rate are calculated and the smaller of the two rates is used for the turbulent combustion (FLUENT, 2006). While a no-slip condition is applied along the wall surface, at the outflow all the physical variables are extrapolated from the internal cells due to the flow being supersonic.

3. Model validation

In order to validate the present numerical method for computing these complex fluid flows in the scramjet combustor with multi-cavities, three computational cases are investigated, namely, the problems of an injection flow, a cavity flow and a fuel-rich combustion flow. The grids for the geometries are structured and generated by the commercial software Gambit, and the grids are distributed more densely near the walls and in the vicinity of the shock wave generation in order to resolve the boundary layers.

3.1 Injection flow

In this first case, the physical model that was experimentally investigated by Weidner et al.(Weidner & Drummond, 1981) is employed since the model has a good two-dimensional structure and it can be used to validate the correctness of the injection phenomenon in the scramjet combustor.

The experimental test investigates the phenomenon of the traverse injection of helium into parallel air flow, namely $\theta=90^\circ$, and the setup of the experiment is schematically shown in Fig. 3. The air stream is introduced from the left hand side of a rectangular channel which is 25.4cm long and 7.62cm high. The static pressure of the air stream is $P=0.0663\text{MPa}$, the static temperature is $T=108.0\text{K}$ and the Mach number is $M=2.9$. The helium is injected at sonic condition from a 0.0559cm slot into an air stream from the bottom surface of the rectangular channel at a location which is 17.8cm downstream from the entrance of the channel. The flow conditions for the helium at the slot exit are $P=1.24\text{MPa}$, $T=217.0\text{K}$ and $M=1.0$.

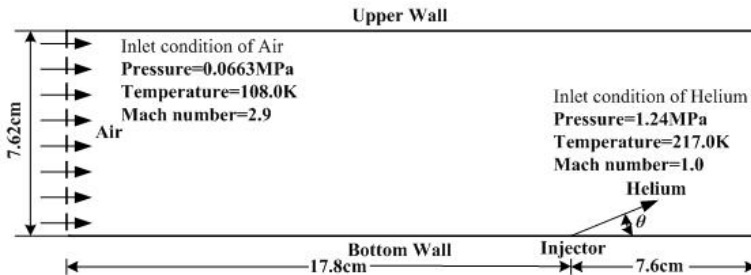


Fig. 3. Schematic of the physical model investigated for injection flow.

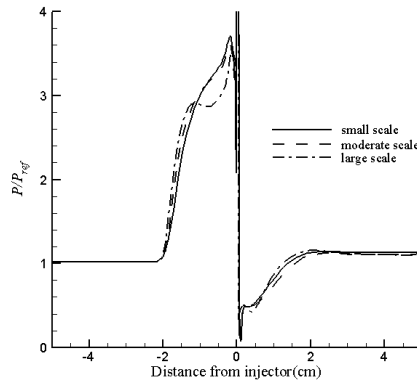


Fig. 4. Static pressure distribution along the bottom wall of the channel for the different grid systems.

In order to investigate grid independency of the numerical simulations, three sets of mesh with different numbers of cells have been employed, namely approximately 19,200, 38,080 and 76,230 cells, respectively. Fig. 4 shows the static pressure distribution along the bottom wall of the channel for the three different grids. It is observed that the shock wave can be captured accurately for all three different grid scales, and the pressure distributions along the bottom wall of the channel in the downstream region of the injection slot are almost the same for the three grids employed. With different grid scales, the location of the disappearance of the reattachment region and the location of the generated shock wave can

be predicted reasonably accurately when compared with the experimental data, see Fig. 5. This means that the difference in the three grid systems employed in the simulations makes only a small difference to the numerical predictions for the interaction between the air stream and the injection.

Fig. 5 shows a comparison between the experimental data and the computational predictions for the pressure along the bottom wall. The reference pressure P_{ref} is 0.0663MPa. It is observed that the computational results obtained in this investigation show good qualitative agreement with the experimental data for both the upstream and downstream regions of the injection.

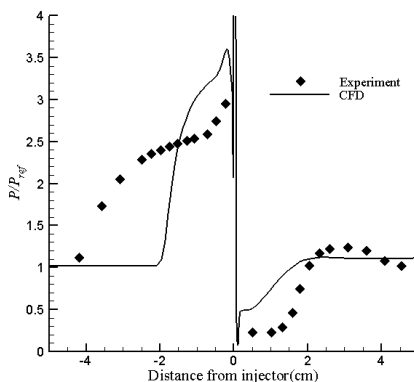


Fig. 5. Comparison between the experimental data of Weidner et al. (Weidner & Drummond, 1981) and the predicted computational pressures along the bottom wall.

Fig. 6 shows a comparison between the experimental data and the predicted computational pressures at a distance of 3.81cm downstream of the injection slot when the reference pressure is 0.21MPa and the reference height is 7.62mm. It is observed that there is a rapid pressure drop at a distance of about 1.524cm (i.e. $y/h=0.2$) from the bottom wall, and this is the location where the separated region disappears downstream of the injection slot. This rapid pressure drop is followed by a pressure rise in the central region of the channel, and this is the intersection point between the shock wave and the transverse line at this location. At the same time, we observe that there are also some discrepancies between the experimental data and the calculated results because of the complex flow field in the vicinity of the injection exit and the inaccuracy of the $k-\epsilon$ turbulent model to simulate the separation region generated just upstream and downstream of the injector.

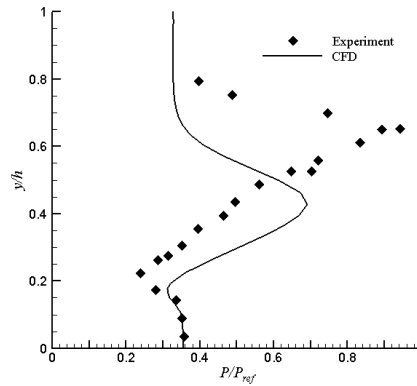


Fig. 6. Comparison between the experimental data of Weidner et al. (Weidner & Drummond, 1981) and the computational pressures at a distance of 3.81cm downstream of the injector.

The helium mass fraction distribution at a distance of 3.81cm downstream of the injector, as obtained from the computational model, agrees reasonably well with the experimental data, see Fig. 7, although there is a slight underprediction by the numerical simulation. It should be noted that the height is nondimensionalized by the height of the channel, namely

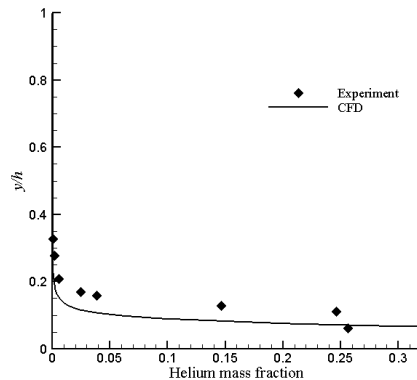


Fig. 7. Comparison between the experimental data of Weidner et al. (Weidner & Drummond, 1981) and the computed value for the helium mass fraction at a distance of 3.81cm downstream of the injector.

$h=7.62\text{cm}$.

From the results presented in Figs. 5, 6 and 7, it is found that the mathematical and computational model can reasonably accurately simulate the interaction between the air stream and the injection. In particular, the model can capture the shock wave and predict the parametric distribution. Therefore we conclude that the mathematical and computational model can be used with confidence to investigate the flow field of the scramjet combustor.

3.2 Cavity flow

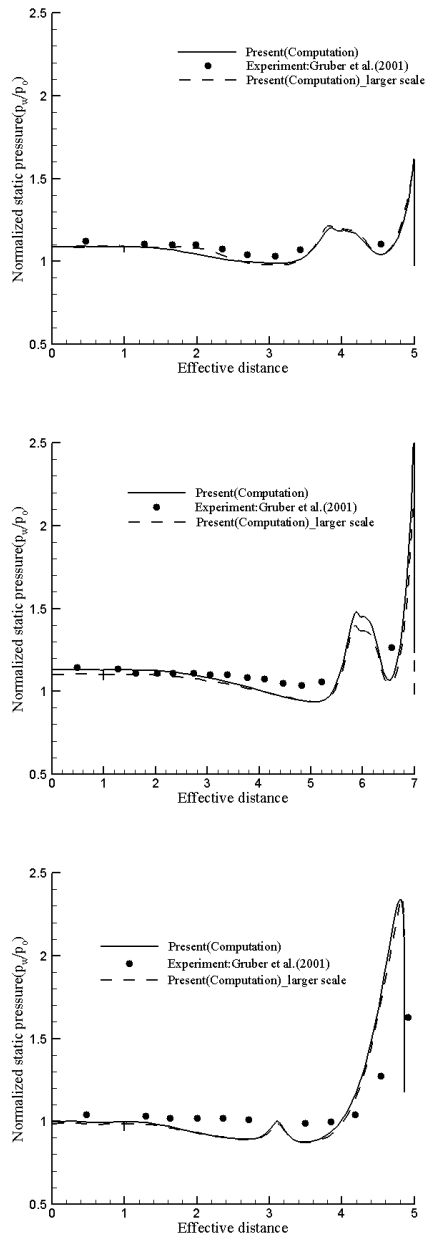


Fig. 8. Wall static pressure distributions for: (a) $L/D=3$ and no swept angle; (b) $L/D=5$ and no swept angle; and (c) $L/D=3$ with the swept angle 30° .

The second model considered follows the experimental work of Gruber et al. (Gruber, Baurle, Mathur, & Hsu, 2001) who studied several cavity configurations for an unheated flow at Mach 3. Cavities with a depth of 8.9mm were used in the experimental work and for the conditions of $L/D=3$, $L/D=5$ without a swept angle, and $L/D=3$ with the swept angle (θ) of 30° , see Fig. 2. In addition, the stagnation temperature (T_0) and stagnation pressure (P_0) of the free stream are 300K and 690kPa, respectively. This physical model is used to validate the correctness of the predicting flow past the cavity flameholder in the scramjet combustor. Fig. 8 shows the wall pressure distributions for $L/D=3$, $L/D=5$ without a swept angle, and $L/D=3$ with the swept angle 30° . Two sets of mesh, with different number of cells, have been employed in order to investigate the grid independency of the numerical simulations, namely approximately 36,400 and 147,200 cells have been employed.

In Fig. 8, the effective distance comprises of the cavity upstream leading edge from the separation corner, the cavity floor and the cavity trailing edge (Kyung *et al.*, 2004). A good agreement is observed between the computed and experimental results, and the difference in the two numbers of grids employed in the simulations produces prediction that makes almost no difference for the unheated cavity flow. We observe that the numerical method employed in this investigation can be used with confidence to simulate the flow field of the scramjet combustor with multi-cavities, and investigate the effect of the fuel injection location on the performance of the scramjet combustor.

3.3 Fuel-rich combustion flow field

The third model considered follows the experimental configuration and flow conditions for the case investigated by Wang Chun et al. (Wang, Situ, Ma, & Yang, 2000), and this model is used to validate the correctness of the combustion model employed in this investigation.

The geometry consists of a straight channel with a length of 370mm followed by a divergent channel with a divergent angle of 3.6° . There is a clapboard between the entrance of the air and the entrance of hot gas, see Fig. 9, and the length of the clapboard is 6mm. All the dimensions used in the CFD model are exactly the same as in the experimental configuration. The air and hot gas flow conditions are presented in Table.3.

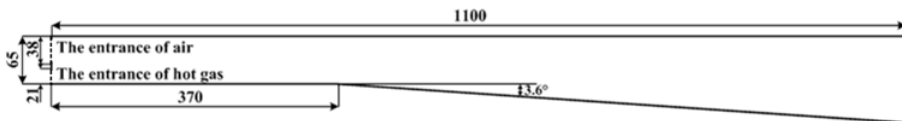


Fig. 9. The geometry of the combustor investigated (Unit: mm)(Wang et al., 2000).

Flow	P_s /MPa	T_s /K	Ma	Mass fraction				
				C_2H_4	O_2	CO_2	H_2O	N_2
Air	0.0977	491.9	2.09	-	0.2330	-	0.0520	0.7150
Hot gas	0.1731	1771.9	1.25	0.1059	0.0103	0.1205	0.1566	0.6067

Table 3. Parameters at the entrance of the supersonic combustor(Wang *et al.*, 2000).

Computational simulations have been performed with a coarse and a fine computational mesh consisting of 8,700 (CFD1) and 16,900 cells (CFD2), respectively. Fig. 10 shows the comparisons of the wall pressure distributions obtained from the present CFD calculations

and the experimental data of Wang Chun et al. (Wang et al., 2000). The solid line represents the numerical results from the coarse mesh, CFD1, and the dashed line is for CFD2. It can be observed that the static pressure distributions on the top and bottom walls obtained by the CFD results show good qualitative agreement with the experimental results. The CFD model captures the shock wave reasonably well in terms of both the location and strength of the wave system. The pressure disturbance on the top and bottom walls is due to the compression and expansion of the flow that occurs alternately in the mixing and expansion sections of the combustor caused by the shock wave system. The pressure disturbance on the top and bottom walls is due to the compression and expansion of the flow that occurs alternately in the mixing and expansion sections of the combustor caused by the shock wave system. At the entrance to the mixing section of the combustor, due to the differences in the flow parameters in the two supersonic flows of air and hot streams, and the effect of the clapboard, the expansion wave appears during flow expansions. When the two flows intersect, the flow direction changes, and the two flows become compressed (Situ, Wang, Niu, Wang, & Lu, 1999). It is concluded that the CFD approach used in this investigation can reasonably accurately simulate these physical phenomena in the scramjet combustor.

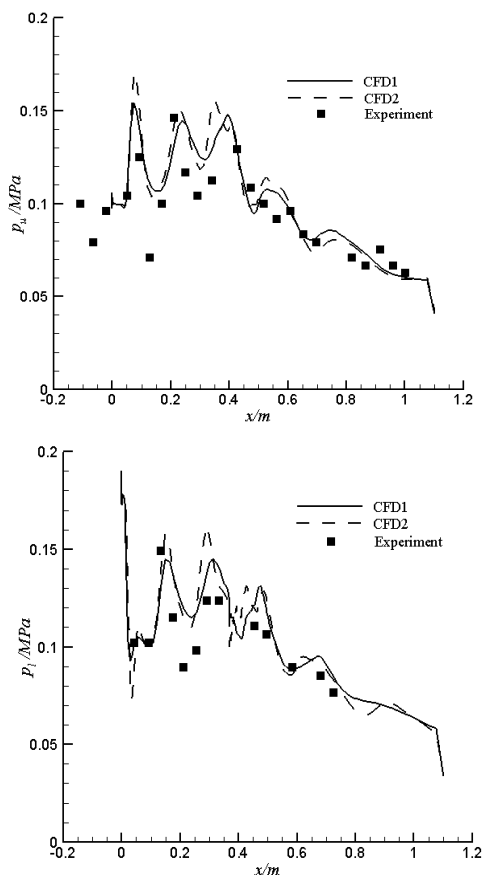


Fig. 10. Wall pressure comparisons of the CFD calculations and the experimental results of Wang Chun et al. (Wang et al., 2000): (a) top wall; and (b) bottom wall.

4. Results and discussion

In order to discuss the influence of the fuel injection location on the flow field of the scramjet combustor with multiple cavity flameholders, three sets of the fuel injection location are employed in this investigation, namely, T_2 , T_4 and both T_2 & T_4 , in Fig. 1. The other fuel injection locations are not considered here, i.e. T_1 or T_3 , because placing the fuel injection location closer to the entrance of the combustor and more concentrated in a certain distance can be of much assistance in the optimization of the performance of the combustor, but the fuel injection location being excessively close to the entrance of the combustor can cause the interaction between the isolator and the combustor to occur more easily and push the shock wave forward, and this will cause the inlet unstart (Wu, Li, Ding, Liu, & Wang, 2007).

Figs. 11-13 show the parametric contours of the cases with the hydrogen injected from T_2 , T_4 and both T_2 & T_4 , respectively. When the hydrogen is injected from both T_2 and T_4 , the shock wave in the combustor is pushed forwards into the isolator by the intense combustion and a high static pressure region formed between the first upper cavity flameholder and the second upper cavity flameholder, see Fig. 13 (a). Then if the fuel injection location moves forward, i.e. T_1 or T_3 , the shock wave is pushed out of the isolator into the inlet and this causes the inlet unstart.

There exists a complex shock wave system in the combustor. When the hydrogen is injected from T_2 , the shock waves generated from the leading edges of the first upper and lower cavity flameholders interact and form a high pressure region, see Fig. 11 (a). At the same time, we observe that the high pressure region exists mainly in the vicinity of the injection due to the fuel combustion. There is a low Mach number region generated on the upper wall of the combustor due to the fuel injection, see Fig. 11 (b). Meanwhile, due to the interaction between the shock wave and the boundary layer, there exists a separation region on the lower wall of the combustor, see Fig. 14 (a). The fuel injection makes the vortices in the cavity flameholder become larger and it deflects into the core flow. The shear layer formed on the leading edge of the second upper cavity flameholder impinges on its trailing edge, and there are almost no vortices in the first upper and lower cavity flameholders. The region in the cavity flameholders acts as a pool to provide the energy to ignite the fuel and prolong the residence time of the flow in the combustor. The Mach number in the cavity flameholders is much lower than that in any other place of the combustor, except in the separation regions, see Fig. 11 (b), and the static temperature in the cavity flameholders is slightly higher than that in the core flow, see Fig. 11 (c). If we change the geometry of the cavity flameholder, it can act as an ignitor in the scramjet combustor, but we should

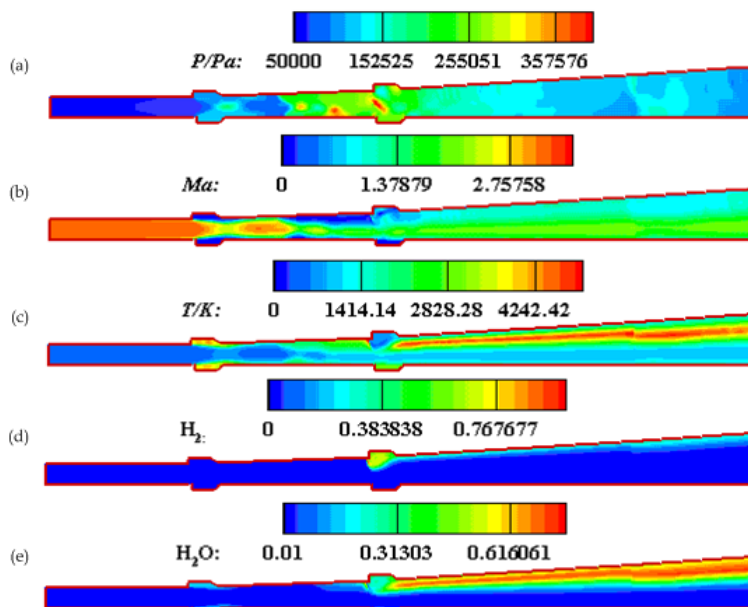


Fig. 11. Parametric contours of the case with hydrogen injected from T_2 : (a) static pressure; (b) Mach number; (c) static temperature; (d) H_2 mass fraction; and (e) H_2O mass fraction.

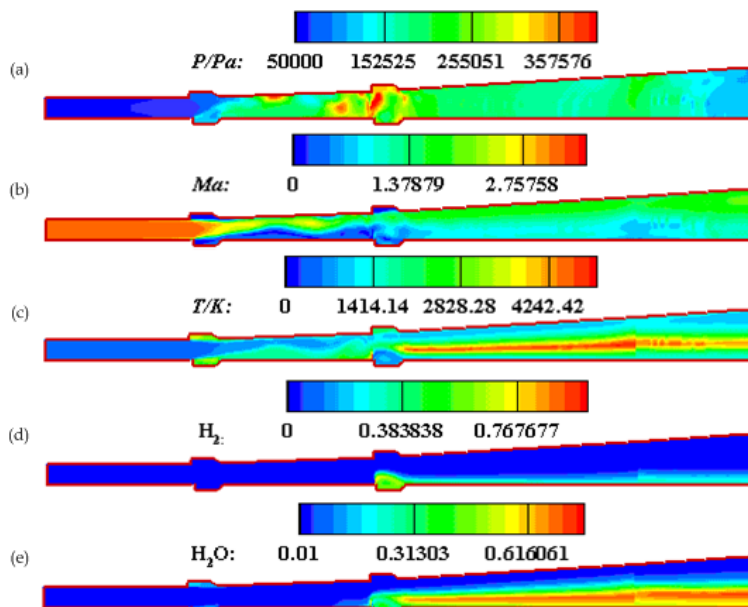


Fig. 12. Parametric contours of the case with hydrogen injected from T_4 : (a) static pressure; (b) Mach number; (c) static temperature; (d) H_2 mass fraction; and (e) H_2O mass fraction.

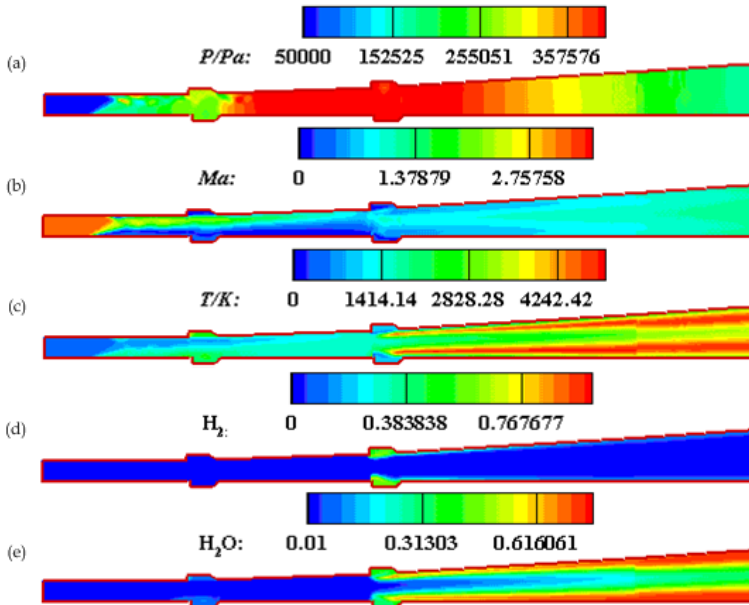


Fig. 13. Parametric contours of the case with hydrogen injected from both T_2 and T_4 : (a) static pressure; (b) Mach number; (c) static temperature; (d) H_2 mass fraction; and (e) H_2O mass fraction.

consider the material of the cavity when operating at such high temperatures. Further, the combustion of the hydrogen takes place near the upper wall of the combustor, see Fig. 11 (d), and the combustion product, namely, H_2O mainly distributes along the upper wall. There is also a small combustion production in the first upper and lower cavity flameholders, see Fig. 11 (e), and it is brought forward by the recirculation zone.

When the hydrogen is injected into the core flow from T_4 , the shock wave generated from the leading edge of the first upper cavity flameholder is much weaker than that generated from the leading edge of the first lower cavity flameholder, and this makes the shock wave, after the interaction, deflect into the upper wall of the combustor. Further, we can observe a high pressure region generated in the vicinity of the upper wall, see Fig. 12 (a), and this is different from the case with the hydrogen injected from T_2 . The reason may lie in the differences in the fuel injection locations. At the same time, we observe two low Mach number regions on the lower wall of the scramjet combustor and this has been caused by the recirculation zones, see Fig. 12 (b) and Fig. 14 (b), and because of the interaction of the shock wave and the boundary layer, there also exists a separation area in the vicinity of the upper wall of the combustor.

Because of the variation in the fuel injection location and the effect of the shock wave, small eddies are formed in both the upper and lower cavities of the first flameholders, and it lies on the rear edge of the cavity, see Fig. 14 (b). The vortices can act as a recirculation zone for the mixture. At this condition, if the fuel is injected from the first staged combustor simultaneously, the performance of the combustor will be improved since the residence time is longer than in the case when the hydrogen is injected from T_2 . Meanwhile, the

distributions of the fuel and the combustion production are opposite to the case when the hydrogen is injected from T_2 , and they mainly distribute along the lower wall of the scramjet combustor because of the fuel injection location, see Fig. 12(d) and (e). Due to the fuel injection being before the cavity flameholder, the eddy generated in the second lower cavity flameholder become larger than before, see Fig. 14 (b), namely the case without fuel injection before the cavity flameholder. The eddy is deflected into the core flow, and the shear layer generated at the leading edge of the second lower cavity flameholder impinges on its trailing edge.

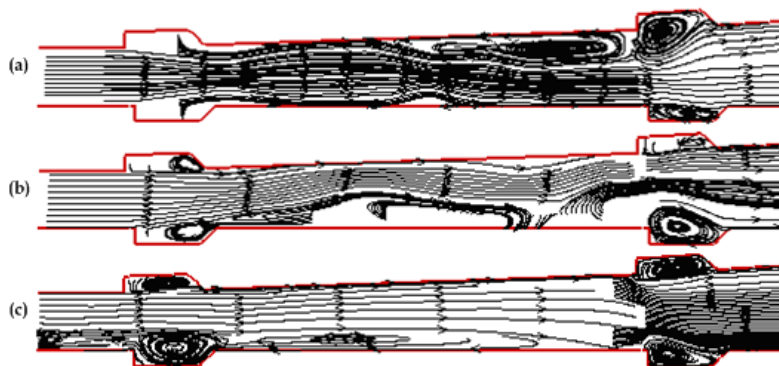


Fig. 14. Streamline distributions in the scramjet combustor with hydrogen injected from different locations: (a) T_2 ; (b) T_4 ; and (c) T_2 and T_4 .

When the hydrogen is injected from both T_2 and T_4 , the flow field is the most complex in the combustor, see Fig. 13. At this condition, the shock wave is pushed out of the combustor because of the intense combustion, and a larger low Mach number region is generated on the lower wall of the combustor because of the stronger interaction between the shock wave and the boundary-layer, see Fig. 13 (b), and it spreads forward to the lower wall of the isolator. A higher static pressure is obtained in the region between the first and the second cavity flameholder, see Fig. 13 (a), and this is the main cause for the spreading forward of the shock wave. Due to the hydrogen injected from both T_2 and T_4 , the fuel and the combustion product distribute both on the upper and lower walls of the combustor, see Fig. 13 (d) and (e), and the combustion occurs mainly in the vicinity of the walls. This illustrates that the injection pressure is not high enough to make the fuel penetrate deeper. The recirculation zone generated at this condition is much larger than that formed in the other two cases, and thus the flow can stay in the combustor much longer, see Fig. 14(c). While travelling over the cavity, the injected hydrogen interacts with the strong trailing edge shock wave, which plays an important role in the combustion. The trailing edge shock wave can improve the static pressure and the static temperature of the flow in the vicinity of the trailing edge of the cavity flameholder, and this can also benefit the combustion.

5. Conclusion

In this chapter, the two-dimensional coupled implicit RANS equations, the standard $k-\epsilon$ turbulence model and the finite-rate/eddy-dissipation reaction model are introduced to simulate the combustion flow field of the scramjet combustor with multiple cavity flameholders. The effect of the fuel injection location on the flow field of the combustor has been investigated. We observe the following:

- The numerical methods employed in this chapter can be used to accurately simulate the combustion flow field of the scramjet combustor, and predict the development status of the shock wave.
- The fuel injection location makes a large difference to the combustion flow field of the scramjet combustor with multiple cavity flameholders. The flow field for the case with hydrogen injected from both T_2 and T_4 is the most complex, and in this situation the shock wave has been pushed forward into the isolator. This causes the boundary layer to separate, generates a large recirculation zone and reduces the entrance region of the inflow. If the fuel injection location moves slightly forward, the shock wave may be pushed out of the isolator, and into the inlet. This will do damage to the inlet start.
- The fuel injection location changes the generation process of the vortices in the cavity flameholders to some extent. When the hydrogen is injected from T_2 , there is no vortex formation in both the upper and lower cavity of the first flameholder. When the hydrogen is injected from T_4 , small eddies are generated in the first upper and lower cavity flameholders. Further, if the hydrogen is injected from both T_2 and T_4 , the eddies in the first upper and lower cavity flameholders become larger, and this is due to the spread of the shock wave pushed by the higher static pressure because of the more intense combustion.
- The fuel injection varies the dimension of the eddy generated in the nearby cavity flameholder. Due to the fuel injection, the eddy generated in the nearby cavity flameholder becomes larger, over the cavity and deflects into the core flow. This makes a larger recirculation zone than the case without fuel injection.
- The cavity is a good choice to stabilize the flame in the hypersonic flow, and it generates a recirculation zone in the scramjet combustor. Further, if its geometry can be designed properly, it can act as an ignitor for the fuel combustion, but the material of the cavity flameholder should be considered for operating at those high temperatures.

6. Acknowledgement

The first author, W Huang would like to express his sincere thanks for the support from the Excellent Graduate Student Innovative Project of the National University of Defense Technology (No.B070101) and the Hunan Provincial Innovation Foundation for Postgraduate (No.3206). Also he would like to thank the Chinese Scholarship Council (CSC) for their financial support (No. 2009611036).

7. References

- Alejandro, M. B., Joseph, Z., & Viswanath, R. K. (2010). Flame stabilization in small cavities. *AIAA journal*, 48(1), 224-235.
- Aso, S., Inoue, K., Yamaguchi, K., & Tani, Y. (2009). A study on supersonic mixing by circular nozzle with various injection angles for air breathing engine. *Acta Astronautica*, 65, 687-695.
- Chadwick, C. R., James, F. D., Kuang-Yu, H., Jeffrey, M. D., Mark, R. G., & Campbell, D. C. (2005). Stability limits of cavity-stabilized flames in supersonic flow. *Proceedings of the Combustion Institute*, 30, 2825-2833.
- Chadwick, C. R., Sulabh, K. D., & James, F. D. (2007). Visualization of flameholding mechanisms in a supersonic combustor using PLIF. *Proceedings of the Combustion Institute*, 31, 2505-2512.
- Daniel, J. M., & James, F. D. (2009). Combustion characteristics of a dual-mode scramjet combustor with cavity flameholder. *Proceedings of the Combustion Institute*, 32, 2397-2404.
- FLUENT, I. (2006). *FLUENT 6.3 User's Guide*. Lebanon, NH: Fluent Inc.
- Gruber, M. R., Baurle, R. A., Mathur, T., & Hsu, K. Y. (2001). Fundamental studies of cavity-based flameholder concepts for supersonic combustors. *Journal of Propulsion and Power*, 17(1), 146-153.
- Gu, H.-b., Chen, L.-h., & Chang, X.-y. (2009). Experimental investigation on the cavity-based scramjet model. *Chinese Science Bulletin*, 54(16), 2794-2799.
- Huang, W., Li, X.-s., Wu, X.-y., & Wang, Z.-g. (2009). Configuration effect analysis of scramjet combustor based on the integral balanceable method. *Journal of Astronautics*, 30(1), 282-286.
- Huang, W., Qin, H., Luo, S.-b., & Wang, Z.-g. (2010). Research status of key techniques for shock-induced combustion ramjet (shcramjet) engine. *SCIENCE CHINA Technological Sciences*, 53(1), 220-226.
- Huang, W., & Wang, Z.-g. (2009). Numerical study of attack angle characteristics for integrated hypersonic vehicle. *Applied Mathematics and Mechanics(English Edition)*, 30(6), 779-786.
- Hyungseok, S., Hui, J., Jaewoo, L., & Yunghwan, B. (2009). A study of the mixing characteristics for cavity sizes in scramjet engine combustor. *Journal of the Korean Society*, 55(5), 2180-2186.
- Jeong, E. J., O'Byrne, S., Jeung, I. S., & Houwong, A. F. P. (2008). Investigation of supersonic combustion with angled injection in a cavity-based combustor. *Journal of Propulsion and Power*, 24(6), 1258-1268.
- Kyung, M. K., Seung, W. B., & Cho, Y. H. (2004). Numerical study on supersonic combustion with cavity-based fuel injection. *International Journal of Heat and Mass Transfer*, 47, 271-286.
- Lauder, B. E., & Spalding, D. B. (1974). The numerical computation of turbulent flows. *Computer Methods in Applied Mechanics and Engineering*, 3(2), 269-289.
- Nardo, A. D., Calchetti, G., Mongiello, C., Giammartini, S., & Rufoloni, M. (2009). *CFD modeling of an experimental scaled model of a trapped vortex combustor*. Paper presented at the ECM 2009 Fourth European combustion meeting, Vienna, Austria.

- Neal, E. H., Michael, K. S., & Allan, P. (2005). *Flight data analysis of HyShot 2*. Paper presented at the 13th AIAA/CIRA International Space Planes and Hypersonic Systems and Technologies Conference, USA.
- Paul, L. M., Vincent, L. R., Luat, T. N., & Jeryl, R. H. (2004). NASA hypersonic flight demonstrators-overview, status, and future plans. *Acta Astronautica*, 55, 619-630.
- Situ, M., Wang, Z.-c., Niu, Y.-t., Wang, C., & Lu, H.-p. (1999). Investigation of supersonic combustion of hydrocarbon fuel-riched hot gas. *Journal of Propulsion Technology*, 20(6), 75-79.
- Sun, M.-b., Geng, H., Liang, J.-h., & Wang, Z.-g. (2009). Mixing characteristics in a supersonic combustor with gaseous fuel injection upstream of a cavity flameholder. *Flow Turbulence Combust*, 82, 271-286.
- Vikramaditya, N. S., & Kurian, J. (2009). Pressure oscillations from cavities with ramp. *AIAA journal*, 47(12), 2974-2984.
- Wang, C., Situ, M., Ma, J.-h., & Yang, M.-l. (2000). Numerical simulation on supersonic combustion of fuel-rich hot gas. *Journal of Propulsion Technology*, 21(2), 60-63.
- Weidner, E. H., & Drummond, J. P. A. (1981). *Parametric study of staged fuel injector configurations for scramjet applications*. Paper presented at the 17th AIAA/SAE/ASME Joint Propulsion Conference, United States.
- Wu, X.-y., Li, X.-s., Ding, M., Liu, W.-d., & Wang, Z.-g. (2007). Experimental study on effects of fuel injection on scramjet combustor performance. *Chinese Journal of Aeronautics*, 20(6), 488-494.